Journal of Luminescence 130 (2010) 2113–2117

Contents lists available at ScienceDirect

Journal of Luminescence

journal homepage: www.elsevier.com/locate/jlumin

Photoluminescence, FTIR and X-ray diffraction studies on undoped and Al-doped ZnO thin films grown on polycrystalline α-alumina substrates by ultrasonic spray pyrolysis

A. Djelloul [a,*], M-S. Aida [b], J. Bougdira [c]

[a] LASPI²A Laboratoire des Structures, Propriétés et Interactions Inter Atomiques, Centre Universitaire Khenchela, Algérie
[b] Laboratoire des Couches minces et Interface, Université de Constantine, Algérie
[c] Institut Jean Lamour, UMR 7198 CNRS, Nancy Université, UPV-Metz, Faculté des Sciences et Techniques, B.P. 239, Bd des Aiguillettes, 54506 Vandoeuvre-lès-Nancy, France

ARTICLE INFO

Article history:
Received 18 October 2009
Received in revised form
13 May 2010
Accepted 10 June 2010
Available online 17 June 2010

Keywords:
Zinc oxide
Zinc aluminate
X-ray diffraction
Infrared spectroscopy
Photoluminescence
Oxygen vacancies

ABSTRACT

Undoped and aluminum-doped zinc oxide (ZnO) thin films have been grown on polycrystalline α-alumina substrates by ultrasonic spray pyrolysis (USP) technique using zinc acetate dihydrate and aluminum chloride hexahydrate (Al source) dissolved in methanol, ethanol and deionized water. A number of techniques, including X-ray diffraction (XRD), scanning electron microscopy (SEM), Fourier transform infrared (FTIR) spectroscopy, and photoluminescence (PL) were used to characterize the obtained ZnO thin films. It was seen that the orientation changed with increase in substrate temperature. During the ZnO deposition Zn source reacted with polycrystalline α-Al_2O_3 substrate to form an intermediate $ZnAl_2O_4$ spinel layer. It has been interestingly found that the intensity of green emission at 2.48 eV remarkably increased when the obtained ZnO:Al films were deposited at 380 °C. The FTIR absorbance intensity of spectroscopic band at $447\pm6\,cm^{-1}$ is very sensitive to oxygen sublattice disorder resulting from non-stoichiometry, which is consistent with the result of PL characterization.

© 2010 Elsevier B.V. All rights reserved.

1. Introduction

ZnO is amongst the most widely studied of all metal oxide systems and has recently become a very popular material due to its great potential for optoelectronics applications and scientific interest. The wide direct band gap of 3.3 eV and large exciton binding energy ~60 meV at room temperature [1] are especially attractive for optoelectronic, nonlinear optics, and electro-optics applications [2]. Aluminum (Al) is a widely used group III dopant, efficiently forming n-type ZnO. Additionally, Al-doped ZnO films are useful materials for a variety of applications, including gas sensors [3], solar cells [4], and flat panel displays [5]. An obvious advantage is that the properties of ZnO can be easily controlled through altering the concentration of oxygen vacancies in them. It has been reported that the PL properties of ZnO are strongly dependent on growth conditions, including growth temperature and growth ambient [6]. Stoichiometric ZnO thin films usually show strong UV luminescence. However, the exact origin of green emission is still a controversial subject, although defects such as oxygen vacancies, oxygen interstitials, zinc vacancies, zinc interstitials, and oxide antisites are suggested as an origin of green PL [7–10]. On introducing an extrinsic dopant Al, the defect environment is altered when an Al atom substitutes a zinc atom. Therefore, it is worth investigating the doping effect on luminescent properties of ZnO:Al. Both FTIR and Raman spectroscopies involve IR wavelength radiation and both measure the vibrational energies of molecules but these methods rely on different selection rules. Changes of oxygen composition can be evaluated indirectly by variation of intensity of the spectroscopic band at $437\,cm^{-1}$ (E_2 (high) mode of hexagonal ZnO) because this mode involves vibrations of only the oxygen sublattice [11]. In this regard, study of the PL and FTIR spectroscopies of ZnO is interesting because it can provide valuable information on the quality and purity of the materials.

In this paper, we present X-ray diffraction, SEM, PL, and FTIR measurements of ZnO thin films deposited on polycrystalline α-alumina substrates by the USP technique. The doping effects of Al on microstructure and optical properties were observed and discussed.

2. Experimental details

ZnO films used in this study were prepared by ultrasonic spray pyrolysis. This technique has many advantages, such as better stoichiometry control, better homogeneity, low processing temperature, lower cost, easier fabrication of large area films, possibility of using high-purity starting materials, and having an

* Corresponding author. Fax: +213 32 33 19 60.
E-mail address: djelloulabdelkader@yahoo.fr (A. Djelloul).

0022-2313/$ - see front matter © 2010 Elsevier B.V. All rights reserved.
doi:10.1016/j.jlumin.2010.06.002

easy coating process of large substrates. The solution used for the films investigated here had the following amounts: 2.2 g $Zn(CH_3COO)_2 \cdot 2H_2O$ (Fulka 99.9%); 50 ml deionized water (resistivity = 18.2 MΩ.cm); 40 ml CH_3OH (Merck 99.5%); and 60 ml C_2H_5OH (Merck 99.5%). Aluminum chloride hexahydrate 1% (Al, at%) $AlCl_3 \cdot 6H_2O$ has been used as the aluminum source. A small amount of acetic acid was added to aqueous solutions to adjust the pH value to about 4.8 to prevent the formation of hydroxides. Water is the most convenient oxidizing agent. Methanol and ethanol were the obvious choice because of their volatility and thus facilitating quick transformation of the precursor mist into vapor form, which is an important criterion for obtaining good quality films. The ultrasonic spraying system used in this work consists of a commercial ultrasonic atomizer VCX 134 AT and a substrate holder with heater. The ultrasonic vibrator frequency was 40 kHz and the power used was 130 W. The median drop size at 40 kHz is 45 μm. The nozzle–substrate distance was 5 cm and during the deposition, the solution flow rate was held constant at 0.1 ml/min. Further details are reported elsewhere [12]. ZnO thin films were deposited onto α-Al_2O_3 polycrystalline substrates ($15 \times 15 \times 1$ mm^3) in the temperature range 330–380 °C. The deposition time was 30 min. The substrate temperature was monitored with a thermocouple and controlled electronically. The film morphology was examined using a (Tescan Vega TS5130MM) scanning electron microscope (SEM). Structural analysis of the ZnO thin films was done by powder X-ray diffraction (XRD) data collected on Seifert XRD 3003-TT diffractometer using CuKα radiation ($\lambda(K\alpha_1) = 0.15406$ nm, $\lambda(K\alpha_2) = 0.15444$ nm). The scan rate (2θ) was 1°/min at the step size of 0.02°. The thickness of thin films was determined using a surface profiler (Dektak 3st). The infrared absorption modes of these films were obtained from FTIR absorbance measurements taken at room temperature using constant powder samples imbedded in KBr pellet of 5 mm diameter. The sample for FTIR measurement was prepared by grinding a thin film scraped from the α-alumina substrate in a synthetic sapphire mortar, pestle and tabletting the ground solid with KBr. The FTIR is performed with a Thermo-Nicolet equipment, in the 4000–400 cm^{-1} region. For oxides all bands have characteristic frequencies between 1000 and 400 cm^{-1}. PL measurement was carried out on a luminescence spectrometer using a Hg arc lamp as the excitation source at room temperature. The excitation wavelength used in PL measurement was 313 nm.

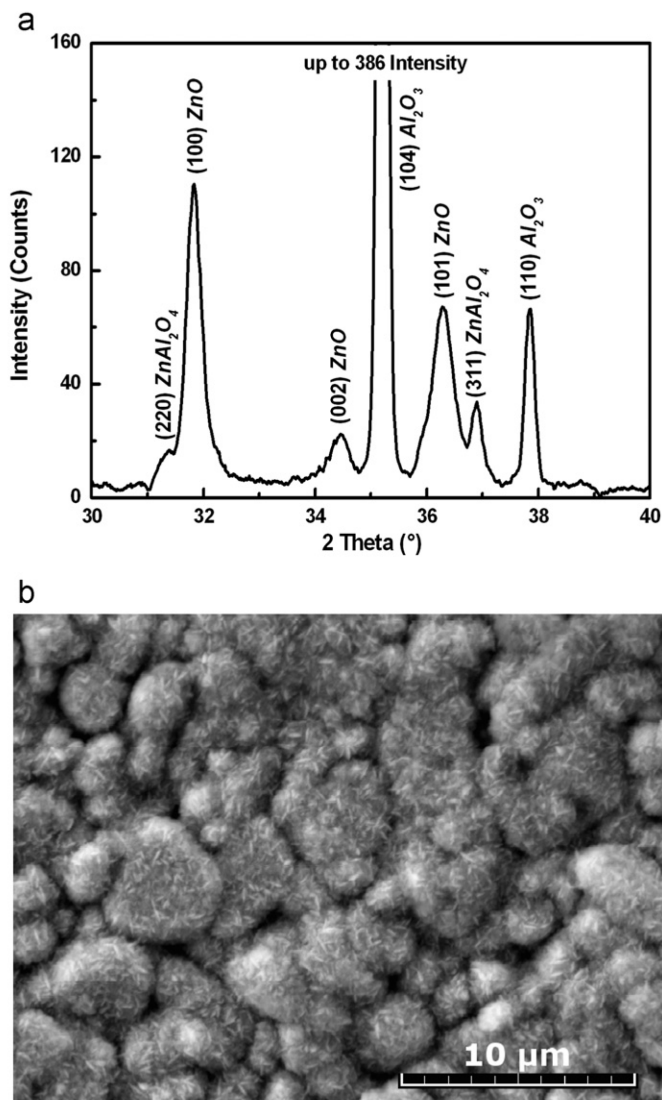

Fig. 1. X-ray diffraction patterns (a) and secondary electron micrographs of ZnO films grown on polycrystalline α-alumina substrate at $T_S = 330$ °C (b).

3. Results and discussion

3.1. Structure and morphology

The X-ray diffraction patterns and SEM micrographs for undoped and Al-doped ZnO films grown on polycrystalline α-alumina substrate are shown in Figs. 1(a) and (b), 2(a) and (b) and 3(a) and(b). The diffraction peaks are easily indexed on the basis of the hexagonal structure of ZnO (P63m/c, $a = 0.3249$ nm and $c = 0.5205$ nm, JCPDS 36-1451), polycrystalline α-Al_2O_3 substrate (R$\bar{3}$C, $a = 0.4758$ nm and $c = 1.2992$ nm, JCPDS 46-1212), and the cubic structure of $ZnAl_2O_4$ (Fd3m, $a = 0.8085$ nm, JCPDS 05-0669). As seen in the XRD pattern, beside the peaks related to the ZnO phase and to the substrate Al_2O_3, a cubic structure of a spinel $ZnAl_2O_4$ phase is also present; the latter originates from the reaction between the deposited film and the substrate; this phase is formed at the interface layer. In order to explore the dependence of structural properties on substrate temperature, we investigated changes in structural characteristics such as crystal structure by means of XRD. The results show that the thin films grown at $T_S = 330$ °C is crystalline since diffraction peak appears in the spectrum corresponding to the strong (1 0 0) and weak planes of the ZnO phase. Raising T_S changed the preferred orientation from (1 0 0) to (0 0 2).

The lattice parameters have been calculated and are summarized in Table 1. The strain along the c-axis, ε_{zz}, is given by the following equation [13]:

$$\varepsilon_{zz} = (c - c_0)/c_0 \times 100\%,$$

where c is the lattice parameter of the strained ZnO films calculated from X-ray diffraction data and c_0 the unstrained lattice parameter of ZnO. According to the above equation the strain can be positive (tensile) or negative (compressive); ε_{zz} values are computed using the above relationship and are summarized in Table 1. The minimum strain value has been found for the ZnO:1%Al film, which is (−)0.169% and the maximum strain value has been found for ZnO films ($T_S = 330$ °C), which is (+)0.151%. The mean crystallite size (D) of the samples was estimated using the Scherrer formula [14]

$$D = \frac{0.94\lambda}{B\cos\theta_B},$$

where λ, θ_B, and B aere the X-ray wavelength, Bragg diffraction angle, and line width at half-maximum, respectively. The characteristic parameters given by X-ray diffraction from the (0 0 2) plane are used to characterize the feature of these

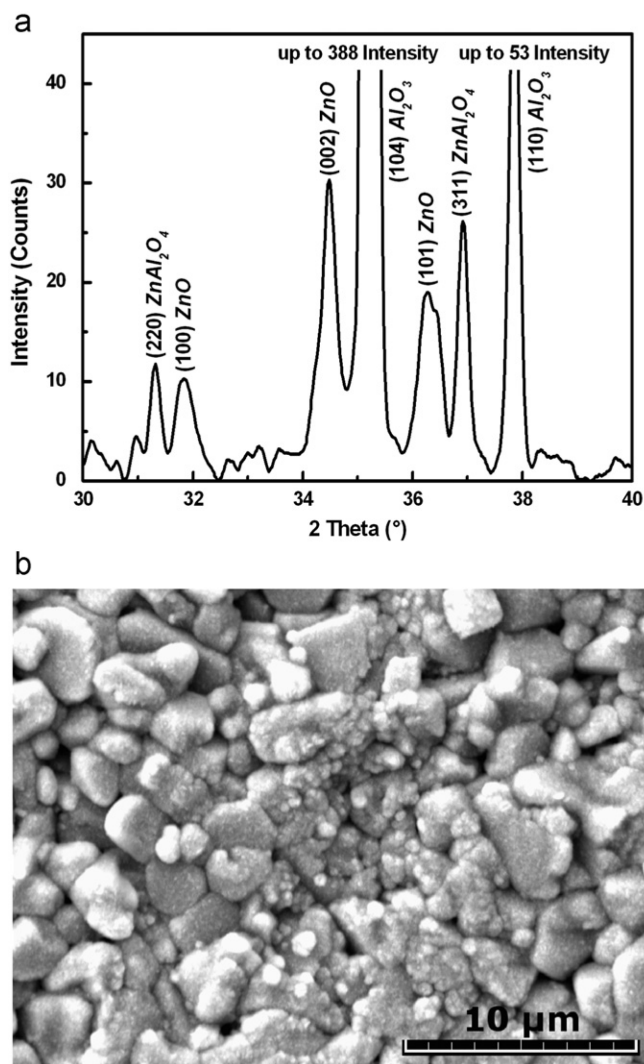

Fig. 2. X-ray diffraction patterns (a) and secondary electron micrographs of ZnO films grown on polycrystalline α-alumina substrate at $T_S = 380$ °C (b).

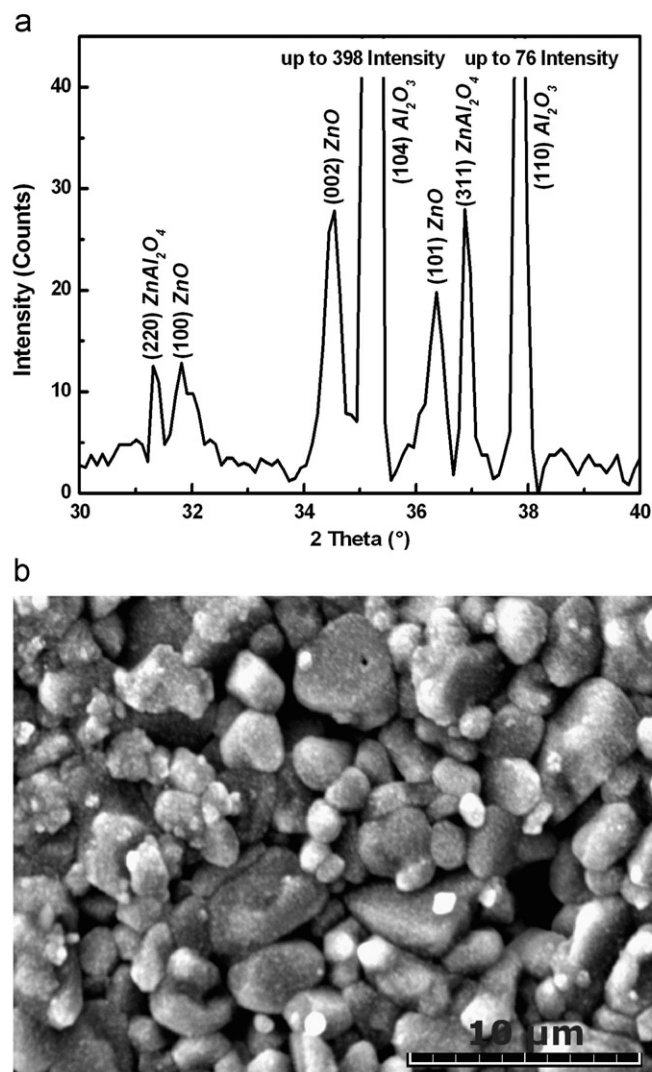

Fig. 3. X-ray diffraction patterns (a) and secondary electron micrographs of ZnO:Al films grown on polycrystalline α-alumina substrate at $T_S = 380$ °C (b).

films. The Bragg diffraction angle, line width at half-maximum, and estimated average crystallite sizes of the films are summarized in Table 1. A small peak shift (0.027°) towards the higher diffraction angle is observed in Al-doped ZnO films compared to the undoped one (34.477°), which may be caused by the fact that the addition of Al is incorporated into ZnO lattice, indicating reduced lattice constant. Since the ionic radius of Zn^{2+} ($r_{Zn}^{2+} = 0.074$ nm) is greater than that of Al^{3+} ($r_{Al}^{3+} = 0.054$ nm), the crystallite size decreases with Al-doping concentration. The mean crystallite size obtained using Scherrer's formula is in all cases substantially smaller than the dimension of grains observed by SEM image, indicating that these grains are probably an aggregation of many crystallites.

The amount of $ZnAl_2O_4$ seems to remain roughly independent of growing temperature and Al doping, the intensity ratio of the peaks of the polycrystalline α-Al_2O_3 substrate, and the spinel phase remaining constant regardless of the substrate temperature, doping, and the growth times. The interesting question that remains is whether the $ZnAl_2O_4$ spinel is a second phase or a single phase. For this, the deposits are made at different times. Fig. 4 shows the observed XRD pattern of the $ZnAl_2O_4$ layer grown on polycrystalline α-alumina substrate at $T_S = 380$ °C. Since the spinel phase is formed at the interface layer between the substrate and the deposited films, to study this phase we need a very thin film. Thereafter, the deposition time was 1 min and its thickness was ~11 nm. The obtained value of the $ZnAl_2O_4$ lattice parameter was $a = 0.8076$ nm. It turns out that this spinel phase is a single stable phase. The mechanism of $ZnAl_2O_4$ spinel formation is proposed as the Zn source (from $Zn(CH_3COO)_2$) reacting with polycrystalline α-Al_2O_3 substrate to form $ZnAl_2O_4$ in the presence of oxygen or water vapor via the following reaction:

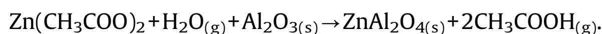
$$Zn(CH_3COO)_2 + H_2O_{(g)} + Al_2O_{3(s)} \rightarrow ZnAl_2O_{4(s)} + 2CH_3COOH_{(g)}.$$

The measured growth kinetics showed that thickness of the $ZnAl_2O_4$ layer can not be larger than 11 nm under the experimental conditions, implying that the in situ produced Zn source can not go very deep into the bulk α-Al_2O_3 substrate, and hence, the reaction can occur only in the α-Al_2O_3 surface regions. Therefore, the reaction is diffusion-limited. The ZnO film was then deposited on the $ZnAl_2O_4$ buffer layer.

3.2. Room temperature photoluminescence analysis

Fig. 5(a) shows representative PL spectra for the three kinds of samples described above, together with that of polycrystalline α-Al_2O_3 substrate for comparison (Fig. 5(b)). When excited by a Hg arc lamp at 313 nm, the as-prepared ZnO shows a strong visible

Table 1
Lattice parameters, strain, ε_{zz}, Bragg diffraction angle, line width at half-maximum, and estimated average crystallite sizes of ZnO films deposited on polycrystalline α-Al_2O_3 substrate at different T_S.

Sample	Lattice parameters (nm)	Strain, ε_{zz} (%)	Thickness (nm)	(0 0 2) peak position, 2θ (deg)	FWHM (deg)	Crystallite size (nm)
ZnO T_S=330 °C	a=0.3245 c=0.5214	0.151	200	34.445	0.236	36.8
ZnO T_S=380 °C	a=0.3247 c=0.5203	−0.067	330	34.477	0.157	55.3
ZnO T_S=380 °C	a=0.3244 c=0.5197	−0.169	250	34.504	0.236	36.8

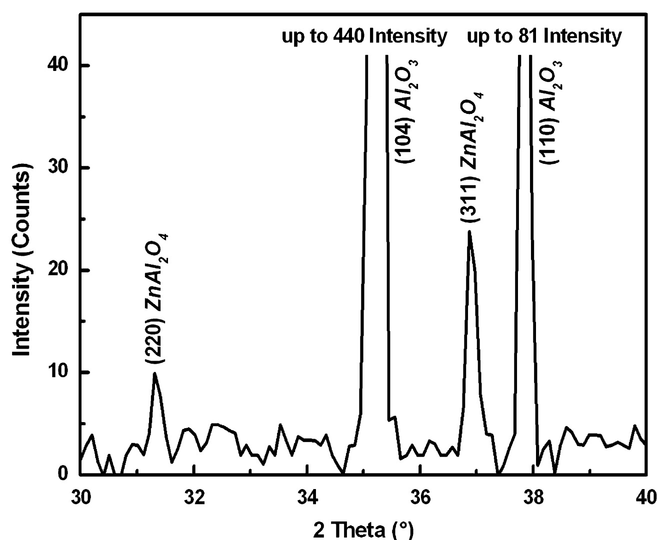

Fig. 4. X-ray diffraction patterns of $ZnAl_2O_4$ films grown on polycrystalline α-alumina substrate at T_S=380 °C; deposit time: 1 min .

emission band at about 2.48 eV (500 nm), which may originate from the commonly assumed recombination of photoexcited holes with electrons occupying the singly ionized oxygen vacancies [15]. As shown in Fig. 5(b), titanium and chromium in α-Al_2O_3 lattice give luminescence in the visible domain. In PL, the narrow band at ~1.86 eV is attributed to chromium impurity, whereas titanium is characterized by a large band centered at ~1.82 eV [16]. Thus, the lines at 1.82 and 1.86 eV are due to the emission of Ti^{3+} and Cr^{3+} in polycrystalline α-Al_2O_3 substrate, respectively. It may be noted here that band edge luminescence was not observed except for undoped ZnO thin films (coarse line) grown at T_S=380 °C. Relative intensity of the defect peak at 2.48 eV decreases slightly with substrate temperature, indicating better crystalline quality of the samples deposited at higher substrate temperatures. This suggests that due to enough thermal energy supplied by increase of growth temperature atoms move to stable sites and that impurities moved to grain boundary. Therefore the defect density of inside grain is diminished and PL properties of ZnO films are improved, whereas the ZnO:Al thin films (fine line) reveal a high concentration of oxygen vacancies because of site competition between Al and Zn atoms. This implies that a high intensity of the green emission band was obtained in ZnO:Al thin films as compared with that of undoped films (coarse line).

3.3. *Fourier transform infrared (FTIR) analysis*

FTIR spectroscopy supplements the information obtained from XRD and SEM. It is the combination of all data that helps us to understand, analyze, and refine more effectively the structure of films. The frequencies at which absorption occurs may indicate the type of functional groups present in the substance. Fig. 6 shows the typical FTIR absorbance spectra of three representative ZnO samples measured at room temperature, together with that of polycrystalline α-Al_2O_3 substrate shown in the inset for comparison. The FTIR spectrum illustrates a series of absorption bands in the range of 400–4000 cm^{-1}. This spectral region encompasses several important stretch modes involving hydrogen bonded to carbon as well as to oxygen and ZnO bondings are clearly represented. An absorption band revealing the vibrational properties of ZnO is observed for each sample in the range 445–453 cm^{-1}. Common bands exist in all cases, such as the broad OH band centered around 3420 cm^{-1} and the 1640 cm^{-1} H_2O vibration band. The very high surface area of these materials results in rapid adsorption of water from the atmosphere because the FTIR samples were kept and ground in air. Theoretical calculations predict O–H vibrations in ZnO ranging from 3216 to 3644 cm^{-1}, depending on the configuration and number of hydrogen atoms in the complex [17]. The hydroxyl results from the hygroscopic nature of ZnO. Three peaks of very weak intensities at 2850, 2920, and 2960 cm^{-1} are observed, which are due to C–H stretching vibrations of alkane groups. These specific peaks correlate well with the observed frequencies of the C–H_2 symmetric stretch (2855 ± 10 cm^{-1}), C–H_2 asymmetric stretch (2926 ± 10 cm^{-1}), and C–H_3 asymmetric stretch (2962 ± 10 cm^{-1}) of saturated hydrocarbons, respectively [18,19]. The absorption at ~2370 cm^{-1} is because of the presence of CO_2 molecules in air. In the FTIR absorbance spectrum of polycrystalline α-Al_2O_3 substrate shown in the Fig. 6 inset, significant spectroscopic bands at 640, 592, and 455 cm^{-1} appear, which are identified to be the characteristic absorption bands of α-Al_2O_3 [20]. Inclusion of Al in the ZnO lattice is confirmed by the emergence of the band at 582 cm^{-1} (fine line), which is identified to be the characteristic absorption band of Al–O stretching mode.

The FTIR results strongly support the hypothesis that at least some of the carbon, oxygen, and hydrogen co-exist as defect complexes in the ZnO thin films and their absorption bands have no obvious change. As can be seen from the peak, intensity of the ZnO bond increased with increasing growth temperature. This was also a strong evidence that undoped ZnO thin films grown at 380 °C had the best crystal quality. Changes of oxygen composition can be evaluated indirectly by variation of intensity of the spectroscopic band at 447 ± 6 cm^{-1} because this mode involves vibrations of only the oxygen sublattice. Since a direct relationship is expected for the spectroscopic band at 447 ± 6 cm^{-1} with the bending mode of oxygen atoms, the intensity of this peak is therefore very sensitive to the oxygen sublattice disorder resulting from non-stoichiometry. According to the IR peak intensity at ~447 ± 6 cm^{-1} of undoped ZnO thin films grown at substrate temperature of 330 and 380 °C and ZnO:Al at 380 °C, it is concluded that the density of oxygen vacancies for ZnO:Al thin films (quite weak intensity) should be much greater than that for

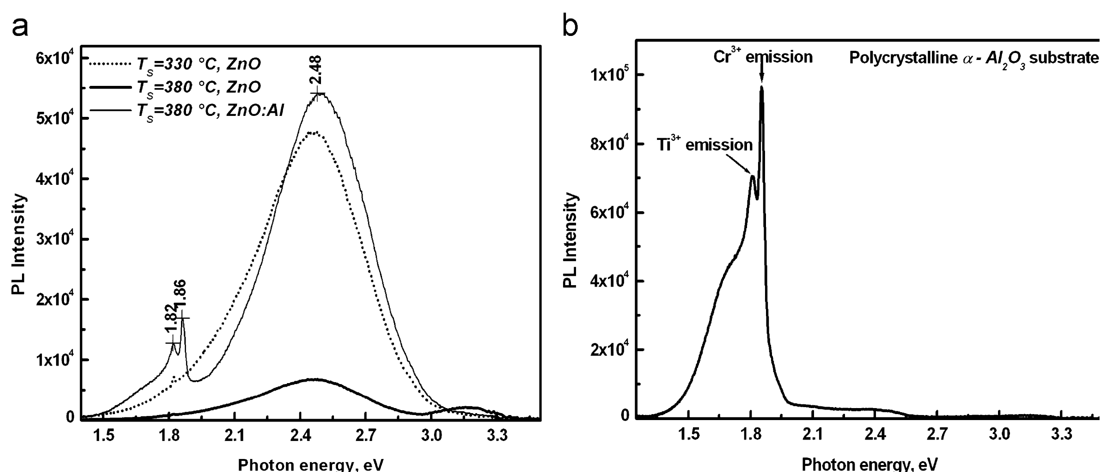

Fig. 5. PL spectra measured at room temperature of undoped and Al-doped ZnO thin films deposited by the USP technique on polycrystalline α-Al_2O_3 substrate at different T_S (a), together with those of polycrystalline α-Al_2O_3 substrate for comparison (b).

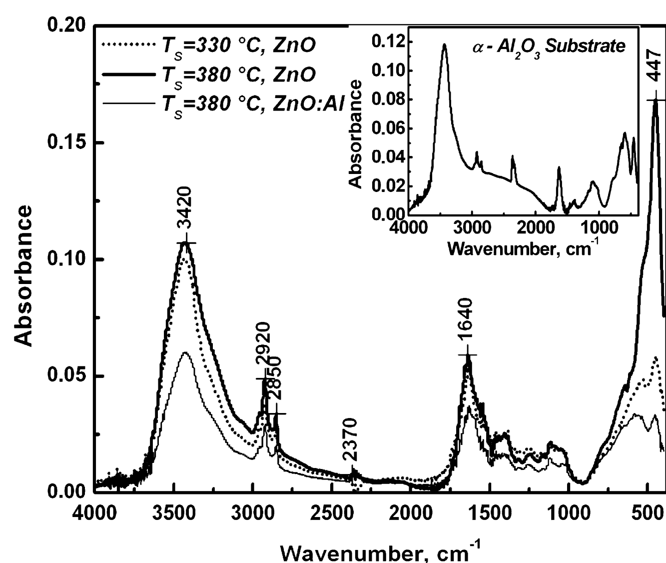

Fig. 6. FTIR absorption spectra of ZnO samples deposited by the USP technique on polycrystalline α-Al_2O_3 substrate at different T_S. The inset shows the FTIR absorbance spectrum of polycrystalline α-Al_2O_3 substrate.

undoped ZnO films, which is consistent with the result of PL characterization. Consequently, PL intensity of green emission ($\sim$2.48 eV) is inversely proportional to FTIR absorbance intensity of the spectroscopic band at $\sim$447 cm^{-1}.

4. Conclusions

In conclusion, undoped and Al-doped ZnO thin films have been grown on polycrystalline α-alumina substrates by the USP technique using zinc acetate dihydrate and aluminum chloride hexahydrate (Al source) dissolved in methanol, ethanol, and deionized water. It was seen that the orientation changed with temperature increase. Structure study of the four samples shows that during the ZnO deposition Zn source reacted with polycrystalline α-Al_2O_3 substrate to form an intermediate spinel $ZnAl_2O_4$ layer. The reaction can occur only in the substrate surface regions. FTIR absorbance intensity of the spectroscopic band at 447 ± 6 cm^{-1} is very sensitive to the oxygen sublattice disorder resulting from non-stoichiometry, which is consistent with the result of PL characterization. It is confirmed that oxygen vacancies are the most important factor that causes the broad visible emission.

References

[1] W.Y. Liang, A.D. Yoffe, Phys. Rev. Lett. 20 (1968) 59.
[2] I.V. Kityk, J. Ebothe, A. Elchichou, M. Addou, A. Bougrine, B. Sahraoui, Phys. Status Solidi B 234 (2002) 553.
[3] J.F. Chang, H.H. Kuo, I.C. Leu, M.H. Hon, Sens. Actuators B 84 (2002) 258.
[4] D. Song, A.G. Aberle, J. Xia, Appl. Surf. Sci. 195 (2002) 291.
[5] M. Chen, Z.L. Pei, C. Sun, J. Gong, R.F. Huang, L.S. Wen, Mater. Sci. Eng. B 85 (2001) 212.
[6] W. Jia, K. Monge, F. Fernandez, Opt. Mater. 23 (2003) 27.
[7] E.G. Bylander, J. Appl. Phys. 49 (1978) 1188.
[8] K. Vanheusden, C.H. Seager, W.L. Warren, D.R. Tallant, J. Caruso, M.J. Hampden-Smith, T.T. Kodas, J. Lumin. 75 (1997) 11.
[9] M. Liu, A.H. Kitai, P. Mascher, J. Lumin. 54 (1992) 35.
[10] B. Lin, Z. Fu, Y. Jia, Appl. Phys. Lett. 79 (2001) 943.
[11] J.M. Calleja, M. Cardona, Phys. Rev. B 16 (1977) 3753.
[12] K. Bouzid, A. Djelloul, N. Bouzid, J. Bougdira, Phys. Status Solidi a 206 (2009) 106.
[13] H.C. Ong, A.X.E. Zhu, G.T. Du, Appl. Phys. Lett. 80 (2002) 941.
[14] B.D. Cullity, Elements of X-Ray Diffraction, 2nd ed., Addison-Wesley, Reading, MA, 1978, pp. 102.
[15] K. Vanheusden, W.L. Warren, C.H. Seager, D.R. Tallant, J.A. Voigt, B.E. Gnade, J. Appl. Phys. 79 (1996) 7983.
[16] M. Ghamnia, C. Jardin, M. Bouslama, J. Electron Spectrosc. Relat. Phenom. 133 (2003) 55.
[17] E.V. Lavrov, J. Weber, F. Börrnert, C.G. Van de Walle, R. Helbig, Phys. Rev. B 66 (2002) 165205.
[18] N.H. Nickel, K. Fleischer, Phys. Rev. Lett. 90 (2003) 197402.
[19] G.-C. Yi, B.W. Wessels, Appl. Phys. Lett. 70 (1997) 357.
[20] A.S. Barker Jr, Phys. Rev. 132 (1963) 1474.